

InBO₃ and ScBO₃ at high pressures: An *ab initio* study of elastic and thermodynamic properties

O. Gomis^{a,*}, H.M. Ortiz^{b,c,d}, J.A. Sans^b, F.J. Manjón^b, D. Santamaría-Pérez^e,
P. Rodríguez-Hernández^f, A. Muñoz^f

^a Centro de Tecnologías Físicas: Acústica, Materiales y Astrofísica, MALTA Consolider Team, Universitat Politècnica de València, 46022 València, Spain

^b Instituto de Diseño para la Fabricación y Producción Automatizada, MALTA Consolider Team, Universitat Politècnica de València, 46022 València, Spain

^c CINVESTAV-Departamento de Nanociencia y Nanotecnología, Unidad Queretaro, 76230 Queretaro, Mexico

^d Proyecto Curricular Licenciatura en Física, Universidad Distrital "Fco. José de Caldas", Bogotá, Colombia

^e Departamento de Física Aplicada-ICMUV, MALTA Consolider Team, Universidad de Valencia, C/Dr. Moliner 50, Burjassot, 46100 Valencia, Spain

^f Departamento de Física, Instituto Univ. de Materiales y Nanotecnología, MALTA Consolider Team, Universidad de La Laguna, 38205 La Laguna, Tenerife, Spain

ARTICLE INFO

Article history:

Received 15 January 2016

Received in revised form

26 May 2016

Accepted 4 July 2016

Available online 5 July 2016

Keywords:

Oxides

Semiconductors

ab initio calculations

High pressure

Mechanical properties

ABSTRACT

We have theoretically investigated the elastic properties of calcite-type orthoborates ABO₃ (A = Sc and In) at high pressure by means of *ab initio* total-energy calculations. From the elastic stiffness coefficients, we have obtained the elastic moduli (*B*, *G* and *E*), Poisson's ratio (*ν*), *B*/*G* ratio, universal elastic anisotropy index (*A_U*), Vickers hardness, and sound wave velocities for both orthoborates. Our simulations show that both borates are more resistive to volume compression than to shear deformation (*B* > *G*). Both compounds are ductile and become more ductile, with an increasing elastic anisotropy, as pressure increases. We have also calculated some thermodynamic properties, like Debye temperature and minimum thermal conductivity. Finally, we have evaluated the theoretical mechanical stability of both borates at high hydrostatic pressures. It has been found that the calcite-type structure of InBO₃ and ScBO₃ becomes mechanically unstable at pressures beyond 56.2 and 57.7 GPa, respectively.

© 2016 Elsevier Ltd. All rights reserved.

1. Introduction

Scandium [1] and indium [2] orthoborates crystallize in the calcite-type structure (space group: *R* $\bar{3}$ c, No. 167, *Z*=6) where Sc (or In) atoms and B atoms are coordinated by 6 and 3 O atoms, respectively (see Fig. 1). Orthoborates have a wide potential for luminescence applications at room conditions. Noteworthy, rare-earth-doped ABO₃ emitting phosphors are known for fifty years [3]. In particular, ScBO₃ and InBO₃ doped with rare-earth ions and transition metals have been studied due to their properties as phosphor or scintillating materials [4–9]. Furthermore, ScBO₃ operates as a room-temperature near-infrared tunable laser when doped with Cr³⁺ [10], and recently it has been found to operate as a Q-switched laser when doped with Yb³⁺ [11]. On the other hand, InBO₃ was postulated as a candidate for neutrino detection [12] and has been confirmed in the last years as a promising

photocatalyst for future applications in treatment of environment contaminants [13–15]. Besides, Eu-doped InBO₃ has been recently found to be a good candidate for highly efficient solar cells [16].

Despite the important technological applications of InBO₃ and ScBO₃, many properties of these borates are unknown. Apart from the well known structure of calcite-type orthoborates, their exceptional luminescence properties, and their mechanical, thermal, radiation-resistant and chemical stability, not many properties are known. In this sense, Raman scattering characterization has been reported for ScBO₃ and InBO₃ [17,18] and the refractive index of InBO₃ has been just recently measured [19]. Besides, the experimental thermal and spectral properties along with the Vickers hardness of Yb³⁺:ScBO₃ have been recently reported [20].

The elastic properties of orthoborates are poorly known and, to the best of our knowledge, only the axial compressibilities and the bulk modulus at zero pressure (*B*₀) are known for ScBO₃ and InBO₃ from a recent experimental and theoretical work [21] along with the experimental Vickers hardness for Yb³⁺:ScBO₃ as stated above [20]. Moreover, while the elastic stiffness coefficients for some calcite-type carbonates have been studied at 1 atm and at high

* Correspondence to: Departamento de Física Aplicada, Escuela Politécnica Superior de Alcoy, Universitat Politècnica de València, Placeta Ferrandiz Carbonell 2, 03802 Alcoy, Alicante, Spain.

E-mail address: osgohi@fis.upv.es (O. Gomis).

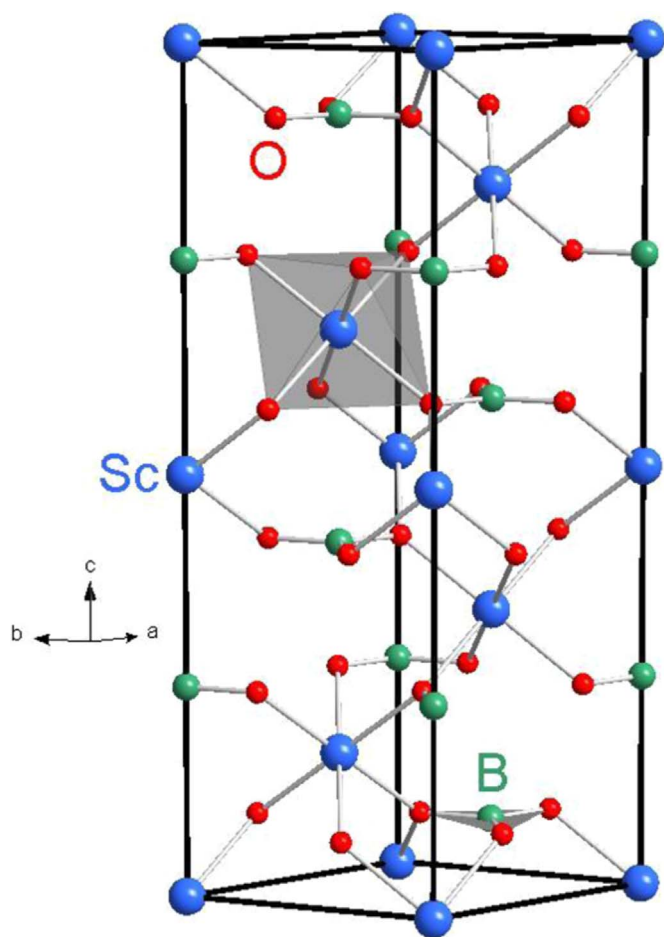


Fig. 1. Calcite-type structure for ScBO_3 . The large (blue) spheres correspond to Sc atoms, the medium (green) spheres to B atoms, and the small (red) spheres to O atoms. (For interpretation of the references to color in this figure legend, the reader is referred to the web version of this article.)

pressures [22–27], no information is available for any calcite-type orthoborate.

In this work, we report a theoretical study of the elastic and thermodynamic properties at 0 GPa and at high pressure (HP) of scandium and indium orthoborates with rhombohedral calcite-type structure. The knowledge of the elastic behavior of the two borates under pressure allows us to discuss the mechanical stability of these calcite-type compounds at high pressures. Elastic and thermodynamic data reported for the two orthoborates can be highly interesting for the comparison with those of calcite-type carbonates in order to understand better the elastic and thermodynamic properties of compounds crystallizing in the important calcite-type structure both at zero and high pressures.

2. Theoretical calculation details

We have performed *ab initio* total-energy calculations within the density functional theory (DFT) [28] using the plane-wave pseudopotential method with the Vienna *ab initio* Simulation Package (VASP) [29]. The projector-augmented wave scheme (PAW) [30] was used as implemented in this package to take into account the full nodal character of the all-electron charge density in the core region. In order to achieve highly converged results and an accurate description of the electronic properties, plane waves up to an energy cutoff of 520 eV were used in the basis set. The exchange–correlation energy was described with the

generalized gradient approximation (GGA) with the PBEsol prescription [31]. A dense Monkhorst–Pack grid ($6 \times 6 \times 6$) of special k-points was used to perform integrations along the Brillouin zone (BZ) to obtain very well-converged energies and forces. The cutoff energy and the k-point sampling employed ensure a high convergence of 1 meV per formula unit in the total energy as well as an accurate calculation of the forces on the atoms. At each selected volume, the structures were fully relaxed to their optimized configuration through the calculation of the forces on atoms and the stress tensor. With this procedure we obtain a set of energies, volumes, pressures, and the related structural parameters. In the relaxed optimized configurations, the forces on the atoms are less than 0.006 eV/Å, and deviations of the stress tensor from a diagonal hydrostatic form are less than 1 kbar (0.1 GPa). The application of DFT-based total-energy calculations to the study of semiconductor properties under HP has been reviewed in Ref. [32], showing that the phase stability, electronic, and dynamical properties of compounds under pressure are well described by DFT.

In order to study the mechanical properties of calcite-type borates by means of *ab initio* calculations we have calculated the elastic constants, which describe the mechanical properties of a material in the region of small deformations; i.e., where the stress-strain relations are still linear. The elastic constants can be obtained by computing the macroscopic stress for a small strain with the use of the stress theorem [33]. Alternatively, they can be also calculated using density functional perturbation theory (DFPT) [34]. In this work, we have evaluated the elastic constants of the calcite-type borates with the use of method implemented in the VASP code: the ground state and fully relaxed structures were strained in different directions taking into account their symmetry [35]. Total-energy variations were evaluated according to a Taylor expansion for the total energy with respect to the applied strain [36]. Due to this fact, it is important to check that the strain used in the calculations guarantees the harmonic behavior. This procedure allows the computation of the C_{ij} elastic constants.

3. Results and discussion

3.1. Elastic properties

The calcite-type structure belongs to the rhombohedral (trigonal) Laue group $\bar{3}m$. This Laue group contains all crystals with $3m$, 32 , and $\bar{3}m$ point groups. In this Laue group, there are 6 independent second-order elastic constants [37] which, in the Voigt notation, are C_{11} , C_{12} , C_{13} , C_{14} , C_{33} and C_{44} [38–41]. Note that $C_{66} = (C_{11} - C_{12})/2$ is not an independent elastic constant [37]. When a non-zero uniform stress is applied to the crystal, the elastic properties are described by the elastic stiffness, or stress-strain, coefficients, which are defined as

$$B_{ijkl} = C_{ijkl} + 1/2 [\delta_{ik}\sigma_{jl} + \delta_{jk}\sigma_{il} + \delta_{il}\sigma_{jk} + \delta_{jl}\sigma_{ik} - 2\delta_{kl}\sigma_{ij}], \quad (1)$$

where C_{ijkl} are the elastic constants evaluated at the current stressed state, σ_{ij} correspond to the external stresses, and δ_{kl} is the Kronecker delta [42–44]. In the special case of hydrostatic pressure ($\sigma_{11} = \sigma_{22} = \sigma_{33} = -P$) applied to a rhombohedral crystal, the elastic stiffness coefficients in the Voigt notation B_{ij} are: $B_{11} = C_{11} - P$, $B_{12} = C_{12} + P$, $B_{13} = C_{13} + P$, $B_{14} = C_{14}$, $B_{33} = C_{33} - P$, $B_{44} = C_{44} - P$, and $B_{66} = C_{66} - P$, where P is the hydrostatic pressure. Note that the B_{ij} and C_{ij} are equal at 0 GPa. When the elastic stiffness coefficients B_{ij} are used, all relationships of the elasticity theory can be applied for the crystal under any loading, including Born's stability conditions which are identical in both loaded and unloaded states [43–47].

Table 1 shows the set of C_{ij} elastic constants at zero pressure obtained from our calculations for both ScBO_3 and InBO_3 . To our

Table 1
 C_{ij} elastic constants (in GPa) for the two calcite-type orthoborates at 0 GPa are given in column C^0 . The linear and quadratic pressure coefficients a and b for the C_{ij} obtained by fitting data to the equation $C_{ij} = C_{ij}^0 + a \cdot P + b \cdot P^2$ are also given. Note that taking into account the definition of the elastic stiffness coefficients B_{ij} from C_{ij} , the linear and quadratic pressure coefficients a_B and b_B for B_{ij} ($B_{ij} = B_{ij}^0 + a_B \cdot P + b_B \cdot P^2$) are given by: $a_B = a - 1$ and $b_B = b$ for B_{11} , B_{33} , B_{44} , and B_{66} ; $a_B = a + 1$ and $b_B = b$ for B_{12} and B_{13} ; and $a_B = a$ and $b_B = b$ for B_{14} .

	ScBO ₃			InBO ₃		
	C^0 (GPa)	a	b ($\times 10^{-2}$ GPa ⁻¹)	C^0 (GPa)	a	b ($\times 10^{-2}$ GPa ⁻¹)
C_{11}	337.4	4.54(3)	-1.06(5)	321.5	5.34(4)	-0.96(8)
C_{12}	134.7	3.67(1)	-0.28(1)	139.0	3.82(1)	-0.07(2)
C_{13}	113.0	3.13(1)	-0.82(2)	113.9	3.52(2)	-1.27(2)
C_{14}	30.3	0.71(1)	-0.39(1)	21.0	0.87(1)	-0.43(2)
C_{33}	205.5	2.50(2)	-0.93(3)	187.8	2.26(3)	-1.03(5)
C_{44}	78.7	1.03(1)	-0.62(2)	68.4	1.14(2)	-0.70(3)
C_{66}	101.3	0.55(1)	-0.71(4)	91.2	0.92(2)	-0.96(6)

knowledge, there are no reported experimental C_{ij} data in these borates to compare with. In particular, C_{11} and C_{33} exhibit the largest values, followed by C_{12} and C_{13} which are similar and smaller than the former, and finally C_{14} is the smallest one. It can be commented that, in general, values for C_{ij} at zero pressure are similar in the two compounds. However, there is a decrease of the value of C_{33} and C_{14} on going from ScBO₃ to InBO₃, and the contrary occurs with C_{12} . The same comments apply for the case of the B_{ij} elastic stiffness coefficients in both compounds as $C_{ij} = B_{ij}$ at 0 GPa. It can be commented that the C_{33}/C_{11} ratio results 0.61 (0.58) for ScBO₃ (InBO₃) at 0 GPa. This ratio describes the longitudinal elastic anisotropy for the single crystal [48] and tell us that the stiffness of ScBO₃ (InBO₃) along the c -axis is 39% (42%) smaller than perpendicular to it. This result is in agreement with chemical arguments since short B–O bonds located at the ab plane perpendicular to the c -axis are less compressible than the long Sc–O and In–O bonds (see Fig. 1) [21]. We have also obtained the axial compressibilities κ_a and κ_c from the elastic constants. The used formulas are [49]:

$$\kappa_a = \frac{C_{33} - C_{13}}{C_{33}(C_{11} + C_{12}) - 2C_{13}^2} \quad (2)$$

$$\kappa_c = \frac{C_{11} + C_{12} - 2C_{13}}{C_{33}(C_{11} + C_{12}) - 2C_{13}^2} \quad (3)$$

Table 2 includes the values for κ_a and κ_c , obtained at 0 GPa using (Eqs. (2) and 3), which are in good agreement with those reported in Ref. [21] obtained from equation of state fits which are also included in Table 2 for comparison. This result gives us confidence about the correctness of our elastic constants calculations. Another quantity to measure the degree of elastic anisotropy of a rhombohedral single crystal is the ratio between the axial compressibilities, κ_c/κ_a [50]. The κ_c/κ_a ratio is 2.67 (3.15) for ScBO₃ (InBO₃) at 0 GPa. This result shows that κ_c is greater than κ_a because the c -axis is more compressible than the a -axis. This is in agreement with the C_{33}/C_{11} ratio smaller than 1 and the fact that the B–O bonds located at the ab plane are less compressible than the Sc–O and In–O bonds as stated above.

Figs. 2 and 3 show the pressure dependence of the elastic constants, C_{ij} , and elastic stiffness coefficients, B_{ij} , in ScBO₃ and InBO₃ up to 70 and 69 GPa, respectively. Despite only B_{ij} are meaningful at any pressure, we report also the pressure dependence of C_{ij} because they are the original magnitudes computed by VASP from which B_{ij} are obtained. Table 1 summarizes the linear and quadratic pressure coefficients of C_{ij} for both compounds. In both borates, all C_{ij} show a positive linear pressure coefficient, whereas all B_{ij} except B_{66} exhibit a positive linear pressure coefficient. On the other hand, B_{44} increases up to 7.5 (11.5) GPa in ScBO₃ (InBO₃) and decreases at larger pressures. It is noteworthy

Table 2
 κ_a and κ_c axial compressibilities in ScBO₃ and InBO₃ obtained from the elastic constants along with the κ_c/κ_a ratio at 0 GPa. Values for κ_a and κ_c reported in Ref. [21] are also included for comparison.

Compound	κ_a (10^{-3} GPa ⁻¹)	κ_c (10^{-3} GPa ⁻¹)	κ_c/κ_a	
ScBO ₃	1.29	3.44	2.67	This work
ScBO ₃	1.30(2)	3.40(3)	2.62(2)	Ref. [21] ^a
ScBO ₃	1.13(3)	3.6(3)	3.2(1)	Ref. [21] ^b
InBO ₃	1.22	3.84	3.15	This work
InBO ₃	1.38(3)	3.75(3)	2.72(3)	Ref. [21] ^a
InBO ₃	1.6(2)	3.49(5)	2.2(1)	Ref. [21] ^b

^a Obtained from a Murnaghan equation of state fit to theoretical data.

^b Obtained from a Murnaghan equation of state fit to experimental data.

that the linear pressure coefficient of all elastic constants and elastic stiffness coefficients is greater in InBO₃ than in ScBO₃ except for C_{33} and B_{33} . On the other hand, the quadratic pressure coefficient is negative in all C_{ij} and B_{ij} for both borates.

With the set of B_{ij} for calcite-type borates, standard analytical formulas for the bulk (B) and shear (G) moduli in the Voigt [38], Reuss [51], and Hill [52] approximations, labeled with subscripts V, R, and H, respectively, can be then applied under any loading [53]:

$$B_V = \frac{2B_{11} + 2B_{12} + B_{33} + 4B_{13}}{9} \quad (4)$$

$$G_V = \frac{M + 12B_{44} + 12B_{66}}{30} \quad (5)$$

$$B_R = \frac{c^2}{M} \quad (6)$$

with

$$M = B_{11} + B_{12} + 2B_{33} - 4B_{13} \quad (7)$$

and

$$c^2 = (B_{11} + B_{12})B_{33} - 2B_{13}^2 \quad (8)$$

$$G_R = \frac{5}{2} \frac{c^2(B_{44}B_{66} - B_{14}^2)}{3B_V(B_{44}B_{66} - B_{14}^2) + c^2(B_{44} + B_{66})} \quad (9)$$

$$B_H = \frac{B_V + B_R}{2} \quad (10)$$

$$G_H = \frac{G_V + G_R}{2} \quad (11)$$

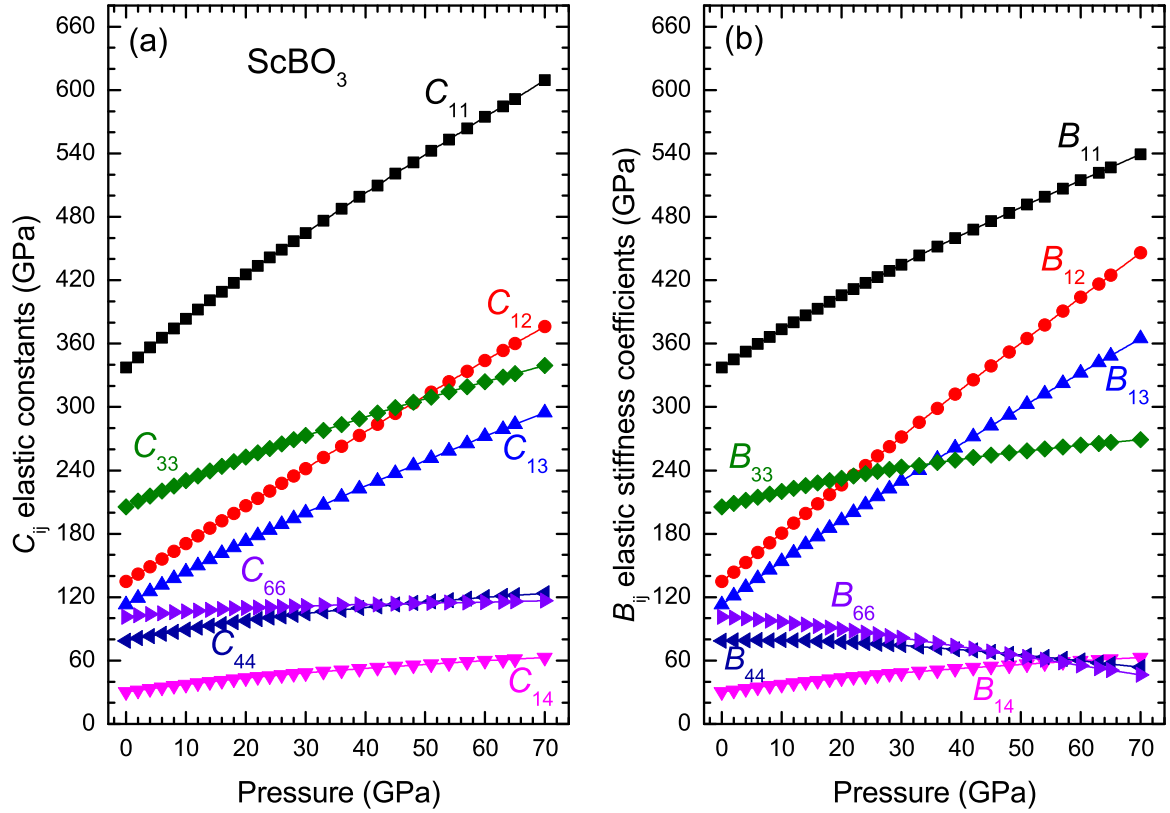


Fig. 2. Pressure dependence of the theoretical elastic constants (a) and elastic stiffness coefficients (b) in ScBO_3 . Solid lines connecting the calculated data points are guides to the eyes.

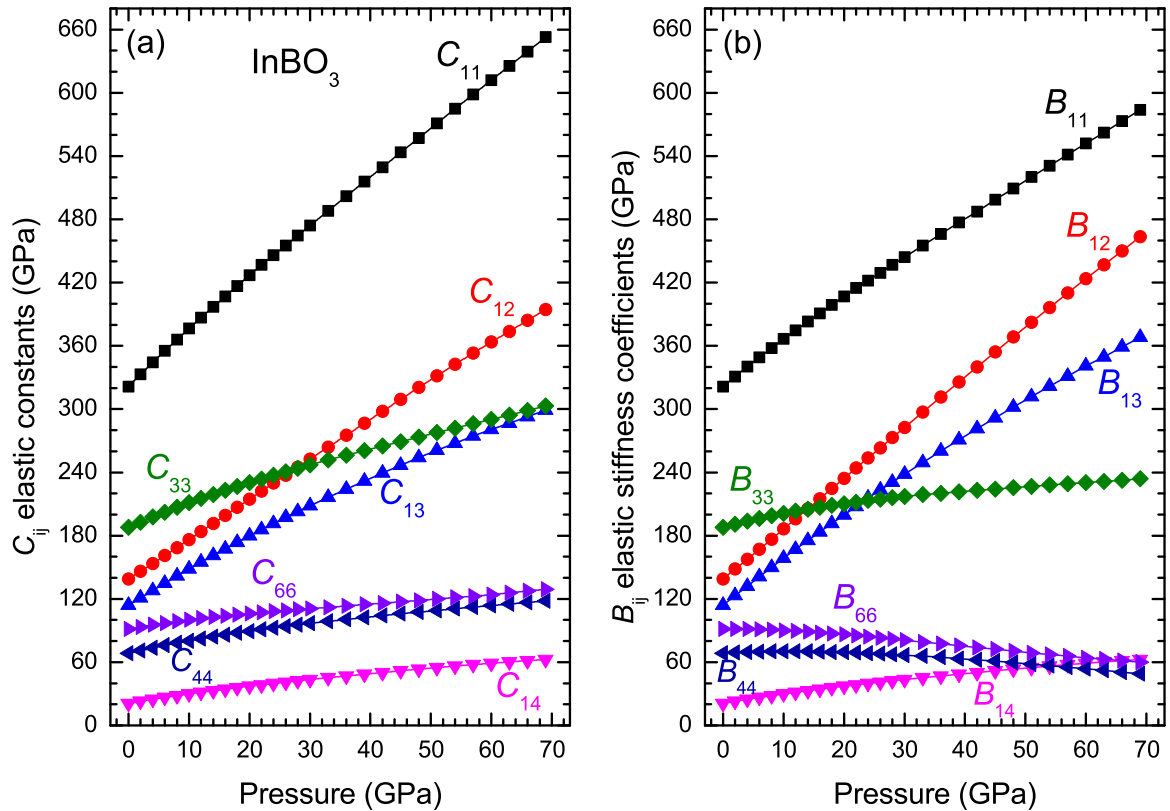


Fig. 3. Pressure dependence of the theoretical elastic constants (a) and elastic stiffness coefficients (b) in InBO_3 . Solid lines connecting the calculated data points are guides to the eyes.

In the Voigt (Reuss) approximation, uniform strain (stress) is assumed throughout the polycrystal [38,51]. Hill has shown that the Voigt and Reuss averages are limits and suggested that the actual effective B and G elastic moduli can be approximated by the arithmetic mean of the two bounds [52]. The Young (E) modulus and the Poisson's ratio (ν) are calculated with the expressions [54,55]:

$$E_X = \frac{9B_X G_X}{G_X + 3B_X} \quad (12)$$

$$\nu_X = \frac{1}{2} \left(\frac{3B_X - 2G_X}{3B_X + G_X} \right) \quad (13)$$

where the subscript X refers to the symbols V , R , and H .

Elastic moduli at 0 GPa for the two calcite-type orthoborates are summarized in Table 3. It is found that the bulk, shear and Young moduli at 0 GPa are larger in ScBO_3 than in InBO_3 ; therefore, the stiffness of ScBO_3 is greater than that of InBO_3 . In fact, the value of the Hill bulk modulus, $B_H = 171.9$ GPa (166.5 GPa) in ScBO_3

Table 3
Elastic moduli B , G , and E (in GPa) and Poisson's ratio (ν) given in the Voigt, Reuss and Hill approximations, labeled respectively with subscripts V , R , and H , in ScBO_3 and InBO_3 at 0 GPa. The B/G ratio and the universal anisotropy index (A_U) are also included.

	ScBO_3	InBO_3
B_V, B_R, B_H	178.0, 165.8, 171.9	173.8, 159.1, 166.5
G_V, G_R, G_H	86.4, 75.8, 81.1	76.5, 69.2, 72.8
E_V, E_R, E_H	223.1, 197.4, 210.2	200.2, 181.2, 190.7
ν_V, ν_R, ν_H	0.29, 0.30, 0.30	0.31, 0.31, 0.31
$B_V/G_V, B_R/G_R, B_H/G_H$	2.06, 2.19, 2.12	2.27, 2.30, 2.29
A_U	0.77	0.63

(InBO_3), is in good agreement with experimental values of $B_0 = 166$ (4) GPa (158(3) GPa) in ScBO_3 (InBO_3), and theoretical values of $B_0 = 167.7$ (6) GPa (160.3(5) GPa) in ScBO_3 (InBO_3), previously reported, which were obtained from fits of experimental and theoretical data to a Birch-Murnaghan equation of state [21]. This agreement is again a check of the goodness of our calculations of the elastic constants. Furthermore, it can be observed that the two calcite-type borates are more resistive to volume compression than to shear deformation ($B > G$) at any pressure.

Table 3 also includes the values of the Poisson's ratio (ν), the ratio between the bulk and shear modulus, B/G , and the universal elastic anisotropy index A_U at 0 GPa. The Poisson's ratio provides information about the characteristics of the bonding forces and chemical bonding. The value of the Poisson's ratio in the Hill approximation is similar in both borates: $\nu = 0.30$ (0.31) in ScBO_3 (InBO_3). This value indicates that the interatomic bonding forces are predominantly central ($\nu > 0.25$) and that ionic bonding is predominant against covalent bonding at 0 GPa [56,57].

The B/G ratio is a simple relationship given by Pugh [58], empirically linking the plastic properties of a material with its elastic moduli. According to the Pugh criterion, a high B/G ratio is associated with ductility, whereas a low ratio corresponds to brittleness. The critical value for the B/G ratio is around 1.75, which separates ductile and brittle materials. In our study, we have found values of B/G at 0 GPa above 1.75 for InBO_3 and ScBO_3 . Therefore, both compounds are ductile at zero pressure, being InBO_3 more ductile than ScBO_3 .

One of the elastic properties of crystals with more importance for both engineering science and crystal physics is the elastic anisotropy, because it is highly correlated to the possibility of inducing microcracks in the materials [59]. This anisotropy can be quantified with the universal elastic anisotropy index A_U [60], which is defined as $A_U = 5(G_V/G_R) + (B_V/B_R) - 6$, where B_V , G_V , B_R and G_R are the bulk and shear moduli in the Voigt and Reuss

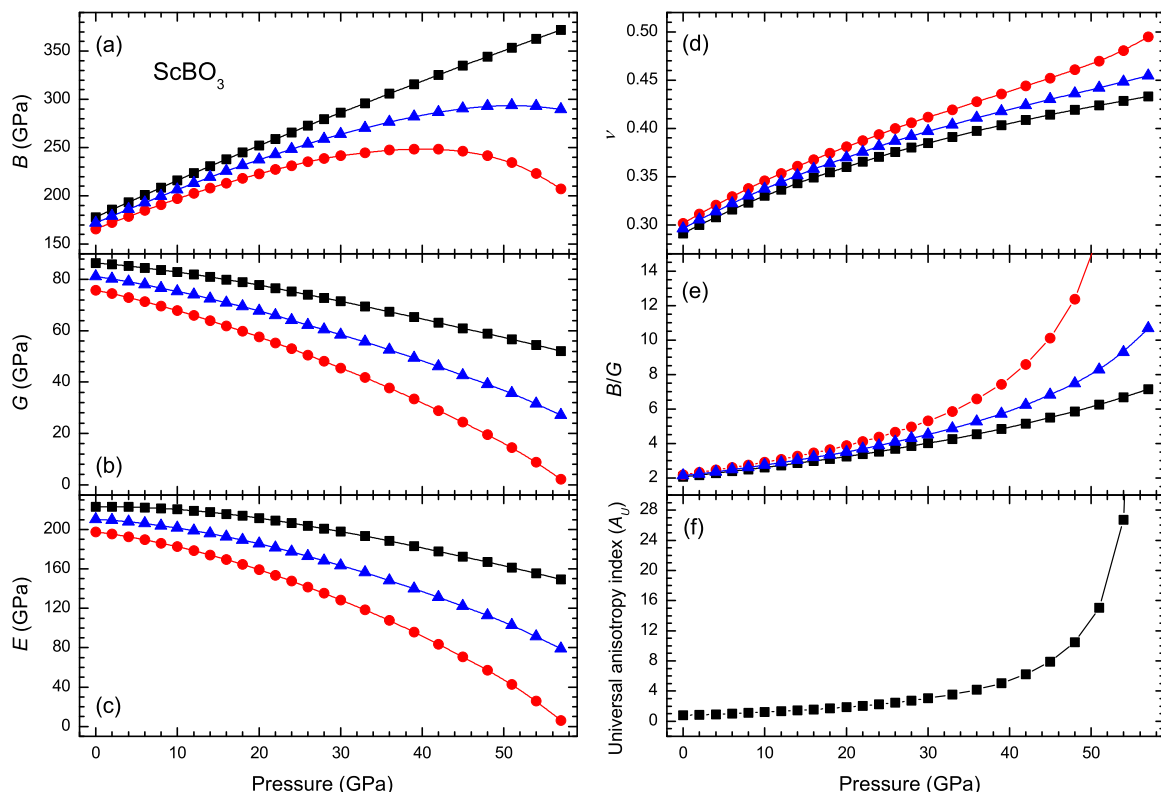


Fig. 4. Pressure dependence of (a) B , (b) G , (c) E , (d) ν , (e) B/G , and (f) A_U in ScBO_3 . Squares, circles, and triangles refer to the Voigt, Reuss, and Hill approximations; respectively. Solid lines connecting the calculated data points are guides to the eyes in panels (a) to (f).

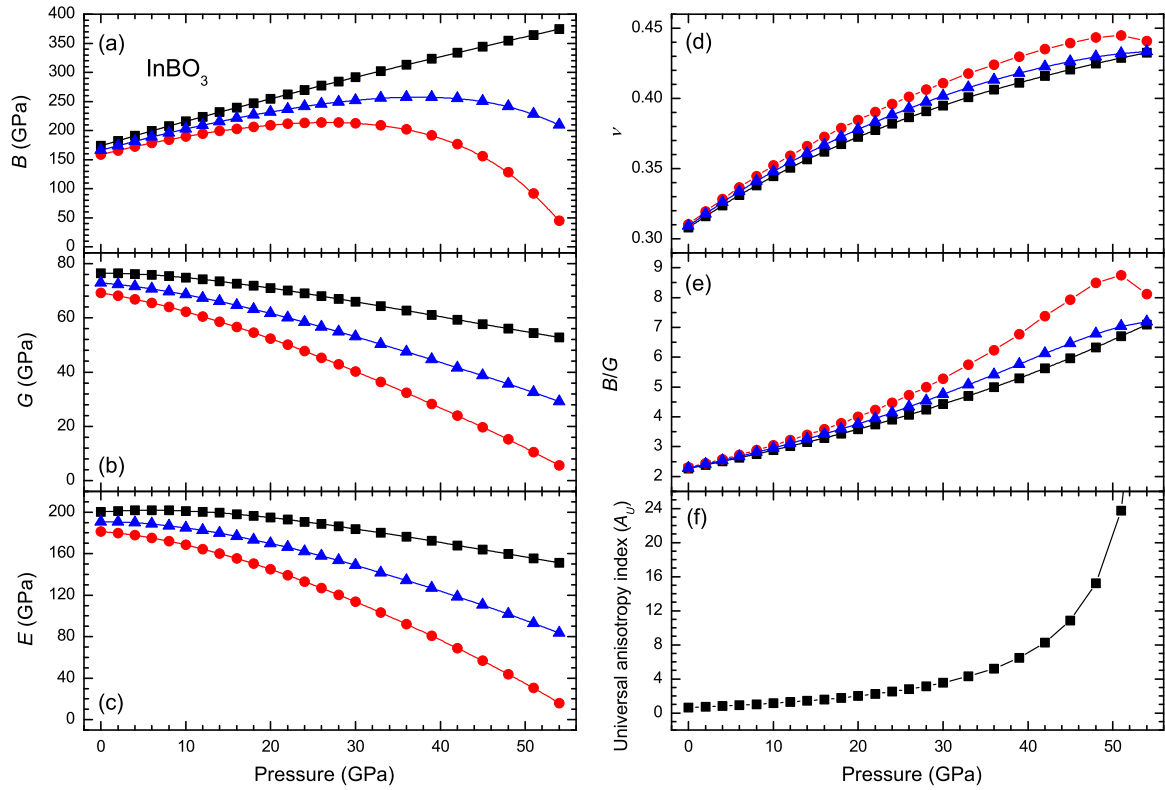


Fig. 5. Pressure dependence of (a) B , (b) G , (c) E , (d) ν , (e) B/G , and (f) A_U in InBO_3 . Squares, circles, and triangles refer to the Voigt, Reuss, and Hill approximations; respectively. Solid lines connecting the calculated data points are guides to the eyes in panels (a) to (f).

approximations, respectively. It is noteworthy that A_U takes into account all the stiffness coefficients B_{ij} by recognizing the tensorial nature of this physical magnitude [60]. If A_U is equal to 0, no anisotropy exists. On the other hand, the more this parameter differs from 0 the more elastically anisotropic is the crystalline structure. The two calcite-type orthoborates have A_U values above 0 at zero pressure; therefore, they are anisotropic, being the anisotropy of InBO_3 slightly smaller than that of ScBO_3 . The elastic anisotropy of both borates reflected by A_U is in agreement with the longitudinal elastic anisotropy given by the C_{33}/C_{11} ratio and the anisotropy in the axial compressibilities given by the κ_c/κ_a ratio, both previously commented.

Figs. 4 and 5 show the pressure dependence of B , G , and E elastic moduli, ν Poisson's ratio, B/G ratio and A_U for ScBO_3 and InBO_3 , respectively. It can be noted that the Hill bulk modulus, B_H , increases with pressure reaching a maximum value of 294 GPa (258 GPa) at 51 GPa (38 GPa) for ScBO_3 (InBO_3) and above that pressure it decreases as pressure increases. Contrarily, the G_H and E_H moduli decrease with pressure for both borates. The Poisson's ratio increases with pressure, reaching a value of 0.45 (0.43) at 54 GPa for ScBO_3 (InBO_3), and indicates an increment of the ductility and of the metallic behavior with increasing pressure. However, we must note that our *ab initio* calculations show that the bandgap of both borates increases with increasing pressure so the increase of the Poisson's ratio is not related with the metallization of the compound at high pressure because of a bandgap closure. Instead, the metallization must be interpreted as a progressive loss of the ionic character of the material related to the increase of atomic coordination and progressive loss of interatomic bond directionality as pressure increases because bond directionality decreases in the series covalent-ionic-metallic. Similarly, the B/G ratio is related to the Poisson's ratio [57] and also increases with pressure in the two borates, thus indicating an increment of the ductility with pressure, reaching a value of 9.3 (7.2) at 54 GPa

Table 4

Vickers hardness (H_v in GPa), longitudinal (v_{lon} in m/s), transverse (v_{trans} in m/s) and averaged (v_m in m/s) elastic wave velocity, Debye temperature (θ_D in K), and minimum thermal conductivity (κ_{min} in $\text{W m}^{-1} \text{K}^{-1}$) in ScBO_3 and InBO_3 at 0 GPa. Data are given in the Voigt, Reuss and Hill approximations indicated with V, R, and H, respectively. The density, ρ , of both borates is also included.

	ScBO_3	InBO_3
H_v (V, R, H)	9.50, 8.10, 8.80	7.81, 7.16, 7.49
v_{lon} (V, R, H)	9210.8, 8788.4, 9002.1	7070.3, 6748.4, 6911.2
v_{trans} (V, R, H)	5000.1, 4684.3, 4844.7	3723.9, 3540.1, 3633.2
v_m (V, R, H)	5578.7, 5233.3, 5408.8	4163.8, 3959.4, 4062.9
θ_D (V, R, H)	771.6, 723.8, 748.1	567.0, 539.2, 553.3
κ_{min} (V, R, H)	1.66, 1.56, 1.61	1.20, 1.14, 1.17
ρ (g/cm^3)	3.455	5.519

in ScBO_3 (InBO_3). Finally, the A_U universal anisotropy factor increases with increasing pressure in ScBO_3 and InBO_3 , thus indicating that the elastic anisotropy increases in both compounds with pressure.

One of the most common elastic properties and less easy to handle is hardness, which is a property generally related to both the elastic and plastic properties of a material. Hardness is an unusual physical property because it is not an intrinsic materials property, but the result of a defined measurement procedure susceptible to precise definitions in terms of fundamental units of mass, length, and time. In practice, hardness is measured by the size of the indentation made on a specimen by a load of a specified shape when a force is applied during a certain time. In this way, there are three principal standard methods for expressing the relationship between hardness and the size of the indentation, these being Brinell, Rockwell, and Vickers. The Vickers hardness, H_v , can be calculated by the formula proposed by Tian et al. [61]:

$$H_v = 0.92(G/B)^{1.137} G^{0.708} \quad (14)$$

We used this formula as it eliminates the possibility of unrealistic negative hardness. The values of H_v for ScBO_3 and InBO_3 at 0 GPa are included in Table 4. ScBO_3 is harder than InBO_3 and both have values of H_v of approximately 8–9 GPa when using elastic moduli in the Hill approximation. Since H_v is smaller than 10 GPa, both compounds can be classified as relatively soft materials. The soft behavior of both orthoborates is correlated with their predicted ductility at zero pressure as previously shown. It must be stressed that the calculated value of $H_v = 8.80$ GPa in the Hill approximation for ScBO_3 is in good agreement with the measured average Vickers hardness for $\text{Yb}^{3+}:\text{ScBO}_3$ of $H_v = 8.19$ GPa [20]. On the other hand, the two orthoborates have theoretical H_v values comparable to that of other ionic oxides such as ZrO_2 with theoretical $H_v \sim 9$ GPa and experimental $H_v = 13$ GPa [62].

Fig. 6 shows the pressure evolution of the Vickers hardness with pressure. It is observed that H_v decreases as pressure increases for both borates. This is related to the fact that the G/B ratio and the G elastic modulus decreases with pressure. In this way, as pressure increases, both borates become softer in good agreement with the increase of their ductility (B/G ratio) as stated above.

Finally, one elastic property which is fundamental for Earth Sciences in order to interpret seismic waves is the average sound velocity, v_m [63]. In polycrystalline materials v_m is given by [64]:

$$v_m = \left[\frac{1}{3} \left(\frac{2}{v_{\text{trans}}^3} + \frac{1}{v_{\text{lon}}^3} \right) \right]^{-1/3} \quad (15)$$

where v_{trans} and v_{lon} are the transverse and longitudinal elastic wave velocities of the polycrystalline material which are given by:

$$v_{\text{lon}} = \left(\frac{B + \frac{4}{3}G}{\rho} \right)^{1/2} \quad (16)$$

$$v_{\text{trans}} = \left(\frac{G}{\rho} \right)^{1/2} \quad (17)$$

where B and G are the elastic moduli and ρ the density. Values of the density and wave velocities v_m , v_{lon} and v_{trans} at 0 GPa are given for the two orthoborates in Table 4. Wave velocities are greater for ScBO_3 than for InBO_3 because of the higher stiffness and smaller density of ScBO_3 than those of InBO_3 . On the other hand, the average wave velocity for ScBO_3 (5408.8 m/s) is greater than that calculated for isoelectronic calcite-type CaCO_3 (4570 m/s) [65].

Fig. 7 reports the evolution of the elastic wave velocities for both borates. Using elastic moduli in the Hill approximation, the calculated v_{lon} increases with pressure reaching a maximum value of 9290.4 m/s (7171.1 m/s) at 27 GPa (21 GPa) for ScBO_3 (InBO_3) and decreases above that pressure. On the other hand, the corresponding velocities v_{trans} and v_m decrease as pressure increases.

3.2. Thermodynamic properties

The Debye temperature is a fundamental parameter that correlates with many physical properties of solids, such as specific heat, elastic constants, and melting temperature. One of the standard methods to calculate the Debye temperature, θ_D , is from elastic constant data using the semi-empirical formula [64]:

$$\theta_D = \frac{h}{k_B} \left[\frac{3n}{4\pi} \left(\frac{N_A \rho}{M} \right) \right]^{1/3} v_m \quad (18)$$

where h is the Planck's constant, k_B is the Boltzmann's constant, n is the number of atoms in the molecule, N_A is the Avogadro's number, ρ is the density, M is the molecular weight, and v_m is the averaged sound velocity. As reported in Table 4, the values of θ_D at 0 GPa using the Hill approximation are 748.1 (553.3) K in ScBO_3

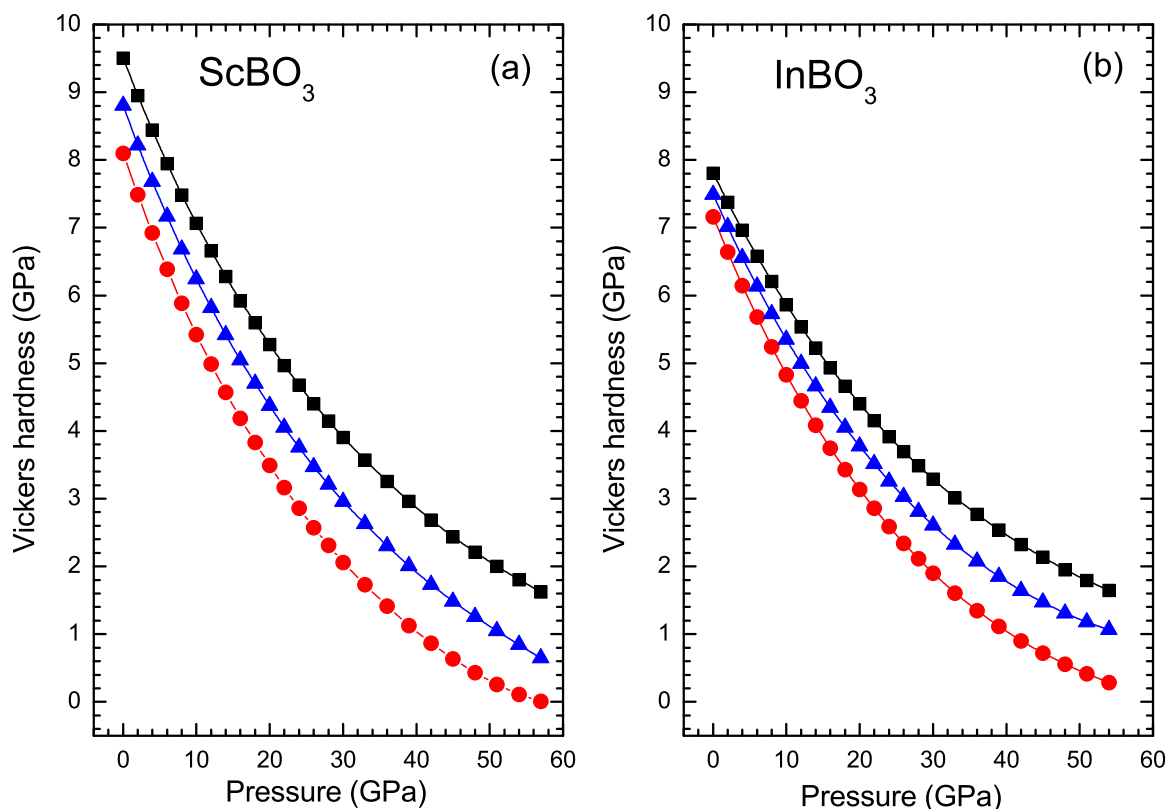


Fig. 6. Evolution with pressure of the Vickers hardness in ScBO_3 (a) and InBO_3 (b). Squares, circles, and triangles refer to the Voigt, Reuss, and Hill approximations, respectively.

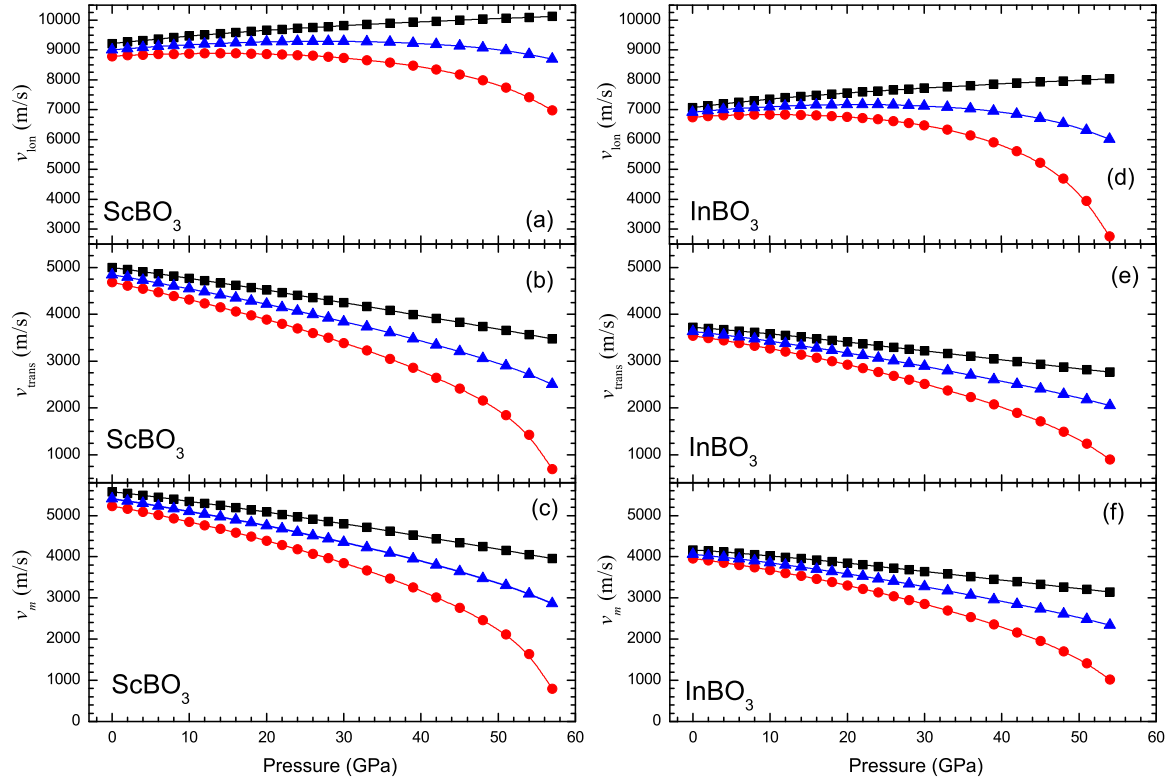


Fig. 7. Pressure dependence of the longitudinal (v_{lon}), transverse (v_{trans}), and average (v_m) elastic wave velocity in ScBO_3 and InBO_3 . Squares, circles, and triangles refer to the Voigt, Reuss, and Hill approximations, respectively.

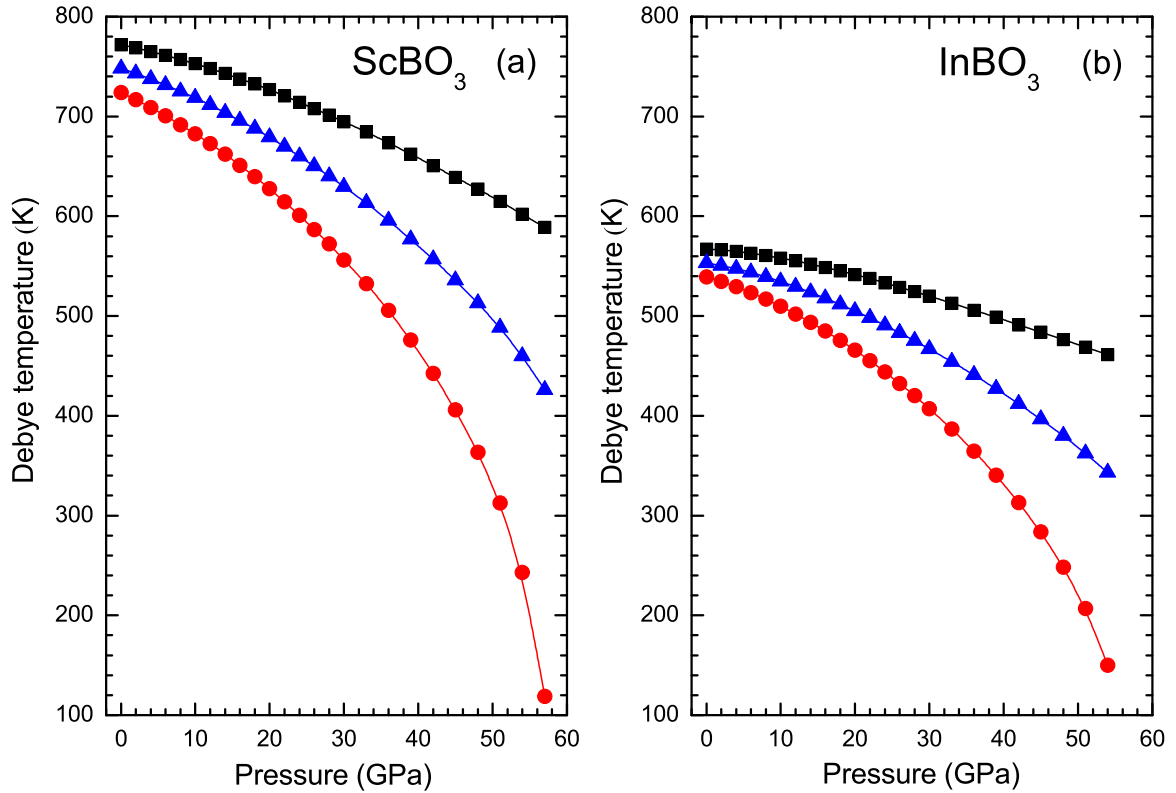


Fig. 8. Evolution with pressure of the Debye temperature in ScBO_3 (a) and InBO_3 (b). Squares, circles, and triangles refer to the Voigt, Reuss, and Hill approximations, respectively.

(InBO_3). We note that the Debye temperature in InBO_3 is slightly greater than that obtained theoretically in calcite-type CaCO_3 (503 K) [65]. Fig. 8 reports the evolution with pressure of the

Debye temperature, θ_D , for both borates. It is observed that θ_D decreases with pressure because v_m decreases with pressure.

The thermal conductivity is the property of a material that

indicates its ability to conduct heat. In order to estimate the theoretical minimum of the thermal conductivity, we have used the following expression [66]:

$$\kappa_{\min} = k_B v_m \left(\frac{M}{n \rho N_A} \right)^{-2/3} \quad (19)$$

The values of κ_{\min} at 0 GPa in ScBO_3 (InBO_3) using the Hill approximation are 1.61 (1.17) $\text{W m}^{-1} \text{K}^{-1}$. Therefore, both borates are low κ materials [67]. It must be stressed that the value of the minimum thermal conductivity in ScBO_3 at 0 GPa is in good agreement (i.e., smaller) with the average thermal conductivity for $\text{Yb}^{3+}:\text{ScBO}_3$ measured at 300 K ($3.3 \text{ W m}^{-1} \text{K}^{-1}$) [20]. Fig. 9 reports the evolution with pressure of the minimum thermal conductivity, κ_{\min} , for both borates. As in the case of θ_D , κ_{\min} decreases with pressure because of the decreasing of v_m with pressure. On the other hand, if we use the simplified formula for κ_{\min} that considers $v_m = 0.87 \sqrt{E/\rho}$ [66], the decreasing of κ_{\min} with pressure is explained by the decreasing of the tensile stiffness of both borates as pressure increases.

3.3. Mechanical stability of the calcite structure

In this section we are going to study the mechanical stability of the calcite-type structure in ScBO_3 and InBO_3 at HP. For that purpose, we will make use of the elastic stiffness coefficients reported in the previous section. The mechanical stability of a crystal at zero pressure can be studied with the Born stability criteria [68]. However, the study of the mechanical stability of a crystal at HP requires the generalization of the Born stability criteria to the case when an external load is applied [69–71]. These generalized stability criteria for trigonal crystals with six independent elastic constants are given by the following conditions:

$$M_1 = B_{11} > 0, \quad (20)$$

$$M_2 = B_{11} - B_{12} > 0 \quad (21)$$

$$M_3 = (B_{11} + B_{12})B_{33} - 2B_{13}^2 > 0 \quad (22)$$

$$M_4 = B_{44}(B_{11} - B_{12}) - 2B_{14}^2 = 2(B_{44}B_{66} - B_{14}^2) > 0 \quad (23)$$

$$M_5 = B_{44} > 0, \quad (24)$$

Fig. 10 shows the pressure dependence of the generalized stability criteria for ScBO_3 and InBO_3 . As it can be observed, our calculations show that all the above criteria are satisfied for the two orthoborates at 0 GPa, thus the calcite-type structure is mechanically stable at 0 GPa. In ScBO_3 , all stability criteria are satisfied at HP except M_4 and M_3 (note that these two criteria are divided by 100 in the figure) which are violated at 57.7 and 69.7 GPa, respectively. Similarly, all stability criteria are satisfied at HP in InBO_3 except M_3 and M_4 which are violated at 56.2 and 59.6 GPa, respectively. In summary, our calculations show that calcite-type ScBO_3 and InBO_3 become mechanically unstable between 56 and 58 GPa.

As regards the mechanical stability of solids, it is interesting to note that the A_U universal anisotropy factor increases quickly at HP when the compound approaches the mechanical instability (see Figs. 4 and 5). On the other hand, M_3 enters the numerator of B_R and G_R (Eqs. (6) and (9)) while $M_4/2$ is in the numerator of G_R (Eq. (9)). Therefore, B_R and G_R moduli for InBO_3 (see Fig. 5) and G_R modulus for ScBO_3 (see Fig. 4) go to zero as pressure approaches to the instability region. HP experimental studies reported to date have not checked the stability of these borates up to those pressures [21].

Finally, we must mention that the structural stability of the calcite-type structure in ScBO_3 on doping has been previously studied. In this way, it has been demonstrated the higher structural stability of the calcite-type structure than the vaterite-type

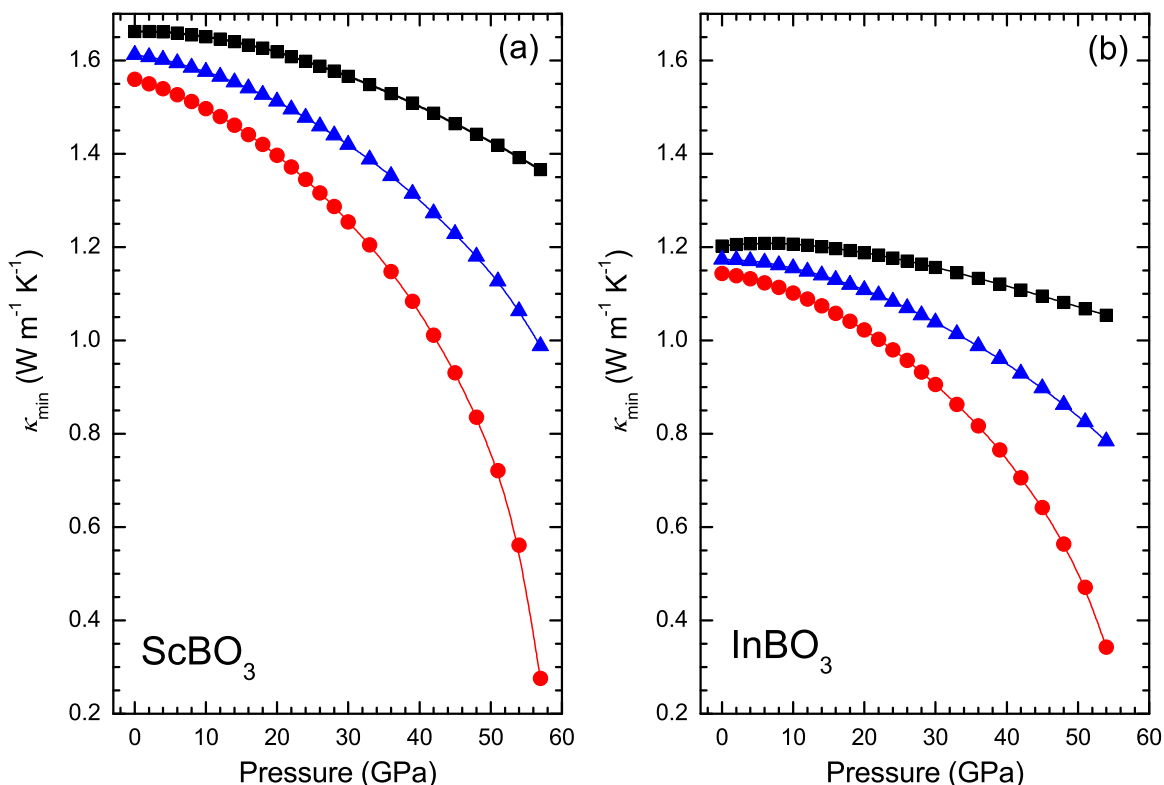


Fig. 9. Evolution with pressure of the minimum thermal conductivity (κ_{\min}) in ScBO_3 (a) and InBO_3 (b). Squares, circles, and triangles refer to the Voigt, Reuss, and Hill approximations, respectively.

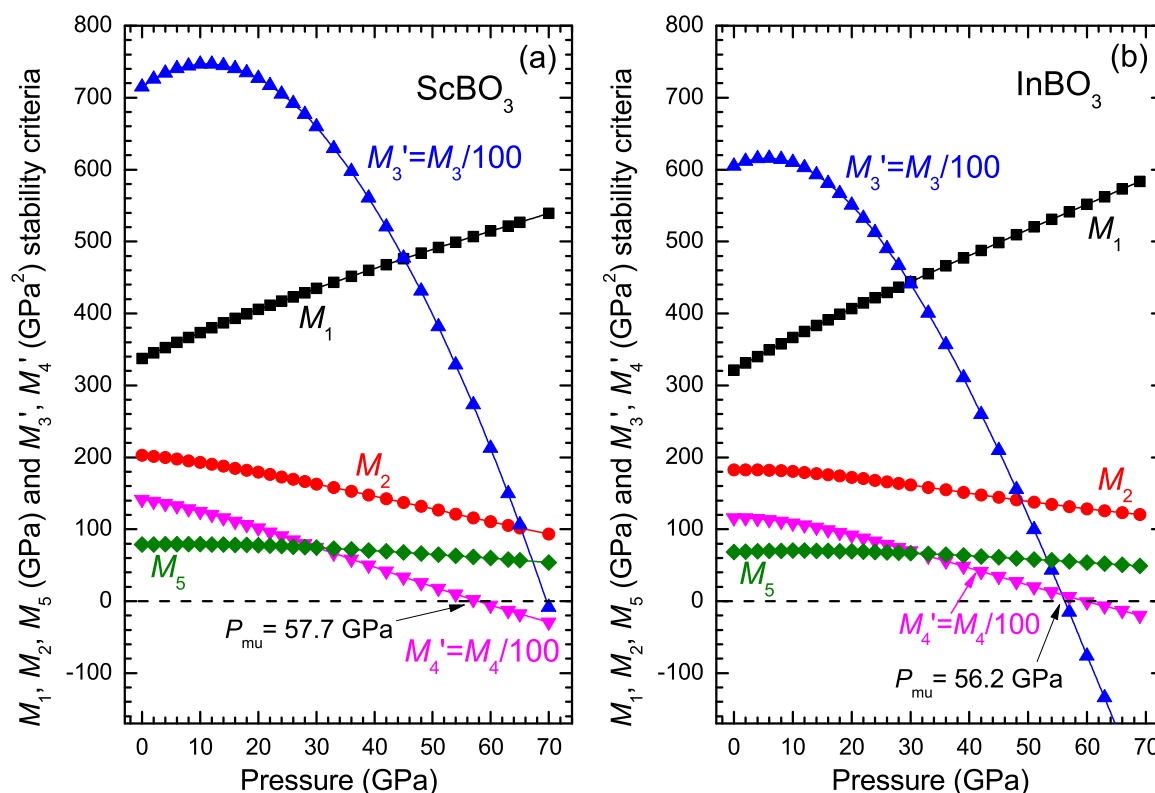


Fig. 10. General stability criteria in ScBO_3 (a) and InBO_3 (b). The pressure P_{mu} at which each borate becomes mechanically unstable is indicated.

structure at room pressure in ScBO_3 when Sc atoms are substituted by Y atoms [72]. However, substitution of Sc atoms in ScBO_3 by much larger Gd and La ions has been found to result in the formation of the huntite-type structure [73]. We hope the present work will foster studies of structural stability of these borates with different dopants and at higher pressures than those already reported.

4. Conclusions

We have theoretically studied the elastic and thermodynamic behavior of two calcite-type orthoborates (ScBO_3 and InBO_3) at high pressure. It has been found that the elastic stiffness coefficients in both borates are similar at 0 GPa. The elastic constants and the elastic stiffness coefficients increase with increasing pressure in all the pressure range except for B_{44} and B_{66} . The evolution with pressure of the B , G , and E elastic moduli, ν Poisson's ratio, B/G ratio and A_U universal elastic anisotropy index is similar in both borates. In this context, both compounds are ductile and more resistive to volume compression than to shear deformation ($B > G$) at all pressures. Furthermore, the elastic anisotropy increases with increasing pressure in both borates. The two borates are relatively soft at 0 GPa and their hardness decreases with increasing pressure. The average elastic wave velocity, Debye temperature and minimum thermal conductivity of both borates decrease with increasing pressure and are lower in InBO_3 than in ScBO_3 . From the behavior of the elastic stiffness coefficients at high pressure we have studied the mechanical stability of the calcite-type structure at high pressure in both compounds and have found that this structure becomes mechanically unstable at 56.2 (57.7) GPa in InBO_3 (ScBO_3).

Acknowledgments

This study is supported by the Spanish MICINN projects MAT2013-46649-C4-2-P/3-P and MAT2015-71070-REDC. H.M.O., A.M., and P.R.H. acknowledge computing time provided by Red Española de Supercomputación (RES) and MALTA-Cluster. J.A.S. acknowledges Juan de la Cierva fellowship program for financial support.

References

- [1] A. Biedl, *Am. Mineral.* 51 (1966) 521–524.
- [2] J.R. Cox, D.A. Kezzler, *Acta Cryst. C* 50 (1994) 1857–1859.
- [3] F.J. Avella, O.J. Sovers, C.S. Wiggins, *J. Electrochem. Soc.* 114 (1967) 613–616.
- [4] E.W.J.L. Oomen, L.C.G. van Gorkom, W.M.A. Smit, G. Blasse, *J. Solid State Chem.* 65 (1986) 156–167.
- [5] G. Blasse, G.J. Dirksen, *Inorg. Chim. Acta* 145 (1988) 303–308.
- [6] G. Blasse, J.P.M. Van Vliet, J.W.M. Verwey, R. Hoogendam, M. Wiegel, *J. Phys. Chem. Solids* 50 (1989) 583–585.
- [7] G. Blasse, C. de Mello Donegá, N. Efryushina, V. Dotsenko, I. Berezovskaya, *Solid State Commun.* 92 (1994) 687–688.
- [8] M. Balcerzyk, Z. Gontarz, M. Moszynski, M. Kapusta, *J. Lumin.* 87 (2000) 963–966.
- [9] J. Thakur, D.P. Dutta, H. Bagla, A.K. Tyagi, *J. Am. Ceram. Soc.* 95 (2012) 696–704.
- [10] S.T. Lai, B.H.T. Chai, M. Long, R.C. Morris, *J. Quantum Elect.* 22 (1986) 1931–1933.
- [11] D. Lu, Z. Pan, R. Zhang, T. Xu, R. Yang, B. Yang, Z. Liu, H. Yu, H. Zhang, *J. Wang, Opt. Eng.* 55 (2016) 081312.
- [12] J.P. Chaminade, A. Garcia, M. Pouchard, C. Fouassier, B. Jacquier, D. Perret-Gallix, L. Gonzalez-Mestres, *J. Cryst. Growth* 99 (1990) 799–804.
- [13] Q. Jia, Y. Miesaki, K. Saito, H. Kobayashi, A. Kudo, *B. Chem. Soc. Jpn.* 83 (2010) 1275–1281.
- [14] J. Yuan, Q. Wu, P. Zhang, J. Yao, T. He, Y. Cao, *Environ. Sci. Technol.* 46 (2012) 2330–2336.
- [15] Y. Yu, Y. Tang, J. Yuan, Q. Wu, W. Zheng, Y. Cao, *J. Phys. Chem. C* 118 (2014) 13545–13551.
- [16] Z.-W. Chiu, Y.-J. Hsiao, T.-H. Fang, L.-W. Ji, *Int. J. Electrochem. Sci.* 10 (2015) 2391–2399.
- [17] G.G. Bogachev, M.N. Iliev, V. Petrov, *Phys. Stat. Sol. b* 152 (1989) K29–K31.
- [18] Y.K. Voron'ko, B.F. Dzhurinskii, A.E. Kokh, A.A. Sobol', V.E. Shukshin, *Inorg. Mater.* 41, 2005, pp. 984–989.

- [19] O. Medenbach, T. Siritanon, M.A. Subramanian, R.D. Shannon, R.X. Fischer, G. R. Rossman, *Mater. Res. Bull.* 48 (2013) 2240–2243.
- [20] D. Lu, Z. Pan, H. Yu, H. Zhang, J. Wang, *Opt. Mater. Express* 5 (2015) 1822–1833.
- [21] D. Santamaría-Pérez, O. Gomis, J.A. Sans, H.M. Ortiz, A. Vegas, D. Errandonea, J. Ruiz-Fuertes, D. Martínez-García, B. García-Domene, A.L.J. Pereira, F. J. Manjón, P. Rodríguez-Hernández, A. Muñoz, F. Piccinelli, M. Bettinelli, C. Popescu, *J. Phys. Chem. C* 118 (2014) 4354–4361.
- [22] D.P. Dandekar, *Phys. Rev.* 172 (1968) 873–877.
- [23] D. Vo Thanh, A. Lacam, *Phys. Earth Planet. Int.* 34 (1984) 195–203.
- [24] M. Catti, A. Pavese, E. Apra, C. Roetti, *Phys. Chem. Miner.* 20 (1993) 104–110.
- [25] M.G. Brik, *Physica B* 406 (2011) 1004–1012.
- [26] A. Ayoub, A. Zaoui, A. Berghout, *Comp. Mat. Sci.* 50 (2011) 852–857.
- [27] C.G. Ungureanu, R. Cossio, M. Prencipe, *Calphad* 37 (2012) 25–33.
- [28] P. Hohenberg, W. Kohn, *Phys. Rev.* 136 (1964) B864–B871.
- [29] (a) G. Kresse, J. Hafner, *Phys. Rev. B* 47 (1993) 558–561;
(b) G. Kresse, J. Hafner, *Phys. Rev. B* 49 (1994) 14251–14269;
(c) G. Kresse, J. Furthmüller, *Comput. Mat. Sci.* 6 (1996) 15–50;
(d) G. Kresse, J. Furthmüller, *Phys. Rev. B* 54 (1996) 11169–11186.
- [30] (a) P.E. Blöchl, *Phys. Rev. B* 50 (1994) 17953–17959;
(b) G. Kresse, D. Joubert, *Phys. Rev. B* 59 (1999) 1758–1775.
- [31] J.P. Perdew, A. Ruzsinszky, G.I. Csonka, O.A. Vydrov, G.E. Scuseria, L. A. Constantin, X. Zhou, K. Burke, *Phys. Rev. Lett.* 100 (2008) 136406.
- [32] A. Mujica, A. Rubio, A. Muñoz, R.J. Needs, *Rev. Mod. Phys.* 79 (2003) 863–912.
- [33] N. Chetty, A. Muñoz, R.M. Martin, *Phys. Rev. B* 40 (1989) 11934–11936.
- [34] S. Baroni, S. de Gironcoli, A. Dal Corso, P. Giannozzi, *Rev. Mod. Phys.* 73 (2001) 515–562.
- [35] Y. Le Page, P. Saxe, *Phys. Rev. B* 65 (2002) 104104.
- [36] O. Beckstein, J.E. Klepeis, G.L.W. Hart, O. Pankratov, *Phys. Rev. B* 63 (2001) 134112.
- [37] J.F. Nye, *Physical properties of crystals. Their representation by tensor and matrices*, Oxford University Press, Great Britain, 1957.
- [38] W. Voigt, *Lehrbstch der Kristallphysih*, B.G. Teubner, Leipzig, Germany, 1928.
- [39] J. Bhimasenachar, *Proc. Indian Acad. Sci.* 22 (1945) 199.
- [40] P.J. Reddy, S.V. Subrahmanyam, *Acta Cryst.* 13 (1960) 493–494.
- [41] L. Peselnick, R.A. Robie, *J. Appl. Phys.* 34 (1963) 2494–2495.
- [42] D.C. Wallace, *Thermoelastic Theory of Stressed Crystals and Higher-Order Elastic Constants*, in: F.S. Henry Ehrenreich, D. Turnbull, F. Seitz (Eds.), *Solid State Physics*, vol. 25, Academic Press, New York, 1970, pp. 301–404.
- [43] J. Wang, S. Yip, S.R. Phillpot, D. Wolf, *Phys. Rev. Lett.* 71 (1993) 4182–4185.
- [44] J. Wang, J. Li, S. Yip, S. Phillpot, D. Wolf, *Phys. Rev. B* 52 (1995) 12627–12635.
- [45] Z. Zhou, B. Joós, *Phys. Rev. B* 54 (1996) 3841–3850.
- [46] B.B. Karki, L. Stixrude, R.M. Wentzcovitch, *Rev. Geophys.* 39 (2001) 507–534.
- [47] O.M. Krasil'nikov, M.P. Belov, A.V. Lugovskoy, I. Yu Mosyagin, Yu. Kh Vekilov, *Comput. Mater. Sci.* 81 (2014) 313–318.
- [48] S. Speziale, F. Jiang, Z. Mao, P.J.M. Monteiro, H.-R. Wenk, T.S. Duffy, F. R. Schilling, *Cem. Concr. Res* 38 (2008) 885–889.
- [49] H. Kimizuka, S. Ogata, J. Li, Y. Shibutani, *Phys. Rev. B* 75 (2007) 054109.
- [50] P. Ravindran, L. Fast, P.A. Korzhavyi, B. Johansson, J. Wills, O. Eriksson, *J. Appl. Phys.* 84 (1998) 4891–4904.
- [51] A. Reuss, *Z. Angew. Math. Mech.* 9 (1929) 49–58.
- [52] R. Hill, *Proc. Phys. Soc. Lond. A* 65 (1952) 349–354.
- [53] J.P. Watt, L. Peselnick, *J. Appl. Phys.* 51 (1980) 1525–1531.
- [54] R. Caracas, T.B. Ballaran, *Phys. Earth Planet. Int.* 181 (2010) 21–26.
- [55] Q.J. Liu, Z.T. Liu, L.P. Feng, *Commun. Theor. Phys.* 56 (2011) 779–784.
- [56] V.V. Brazhkin, A.G. Lyapin, R.J. Hemley, *Philos. Mag. A* 82 (2002) 231–253.
- [57] G.N. Greaves, A.L. Greer, R.S. Lakes, T. Rouxel, *Nat. Mater.* 10 (2011) 823–837.
- [58] S.F. Pugh, *Philos. Mag.* 45 (1954) 823–843.
- [59] V. Tvergaard, J.W. Hutchinson, *J. Am. Ceram. Soc.* 71 (1988) 157–166.
- [60] S.I. Ranganathan, M. Ostoja-Starzewski, *Phys. Rev. Lett.* 101 (2008) 055504.
- [61] Y. Tian, B. Xu, Z. Zhao, *Int. J. Refract. Met. H.* 33 (2012) 93–106.
- [62] X.-Q. Chen, H. Niu, D. Li, Y. Li, *Intermetallics* 19 (2011) 1275–1281.
- [63] J.P. Poirier, *Introduction to the Physics of the Earth's Interior*, Cambridge University Press, Cambridge, 2000.
- [64] O.L. Anderson, *J. Phys. Chem. Solids* 24 (1963) 909–917.
- [65] H. Wang, Y. Xu, M. Shimono, Y. Tanaka, M. Yamazaki, *Mater. Trans.* 48 (2007) 2349–2352.
- [66] D.R. Clarke, *Surf. Coat. Technol.* 163 (2003) 67–74.
- [67] C.G. Levi, *Curr. Opin. Solid St. M.* 8 (2004) 77–91.
- [68] M. Born, K. Huang, *Dynamical Theory of Crystal Lattices*, Oxford University Press, London, 1954, p. 140.
- [69] D.C. Wallace, *Phys. Rev.* 162 (1967) 776–789.
- [70] G. Grimvall, B. Magyari-Köpe, V. Ozolinš, K.A. Persson, *Rev. Mod. Phys.* 84 (2012) 945–986.
- [71] H. Wang, M. Li, J. Phys. Condens. Matter 24 (2012) 245402.
- [72] I.M. Shmytko, I.N. Kiryakin, G.K. Strukova, *Phys. Solid State* 53 (2011) 377–385.
- [73] N. Ye, *Structure Design and Crystal Growth of UV Nonlinear Borate Materials in Structure-Property Relationships in Non-Linear Optical Crystals I: The UV-vis region*, *Struct. Bond*, vol. 144, Springer, 2012, pp. 181–222.